Neuronal responses to transient hypoglycaemia in the dorsal vagal complex of the rat brainstem

Robert H. Balfour[1,2], Ann Maria Kruse Hansen[3] and Stefan Trapp[1,2]

[1]*Department of Anaesthetics, Pain Medicine and Intensive Care, Chelsea & Westminster Hospital, Imperial College London, UK*
[2]*Biophysics Section, Blackett Laboratory, Imperial College London, UK*
[3]*Novo Nordisk A/S, Research & Development, Maaloev, Denmark*

Several regions of the mammalian brain contain glucosensing neurones. *In vivo* studies have suggested that those located in the hypothalamus and lower brainstem are involved in glucoprivic feeding and homeostatic control of blood glucose. We have identified and characterized hypoglycaemia-sensitive neurones in the dorsal vagal complex of the brainstem using *in situ* hybridization, single-cell RT-PCR and whole-cell patch-clamp recordings from rat brainstem slices. Approximately 80% of neurones did not respond to hypoglycaemia (changing artificial cerebrospinal fluid (ACSF) glucose from 10 mM to 0 mM) within 5 min (non-responsive: NR). Another 10% depolarized within 155 ± 31 s (mean ± S.E.M.) of glucose removal (glucose-inhibited: GI), and the remaining neurones hyperpolarized within 53 ± 7 s (glucose-excited: GE). The hyperpolarization was reversed by the K_{ATP} channel blocker tolbutamide. Single-cell RT-PCR revealed that GI and GE, but not NR, cells expressed glucokinase (GLK). In contrast, SUR1, a K_{ATP} channel subunit, was expressed in GE and some NR cells. *In situ* hybridization with biotin-labelled riboprobes in the dorsal vagal complex revealed ubiquitous expression of SUR1, and widespread, but sparse, expression of GLK. Identification of astrocytes using a GFAP (glial fibrillary acidic protein) antibody showed that GLK and GFAP were not colocalized. In summary, we have demonstrated that GI and GE neurones exist in the brainstem and that GLK is essential for their function. It seems likely that GE neurones work in a way analogous to pancreatic β-cells in that they require both GLK and K_{ATP} channels.

(Resubmitted 15 September 2005; accepted 7 November 2005; first published online 10 November 2005)
Corresponding author S. Trapp: Biophysics Section, Blackett Laboratory, South Kensington Campus, Imperial College London, London SW7 2AZ, UK. Email: s.trapp@imperial.ac.uk

Insufficient release of insulin in response to a rise in blood glucose levels is a key feature of diabetes mellitus. In type II diabetes mellitus this is usually attributed to either a defect in insulin action or defective stimulus–secretion coupling in pancreatic β-cells. However, neither of these ideas takes into account any neuronal influence on β-cell function, such as the innervation by vagal fibres. The importance of this projection is highlighted by the dependence of the cephalic phase of insulin release on an intact vagal nerve (Berthoud & Powley, 1990). One hundred and fifty years ago, Claude Bernard reported that puncture lesions of the medulla oblongata caused diabetes mellitus (Bernard, 1855), providing the first evidence that the brainstem is involved in the control of blood glucose. More than one hundred years later, Laughton & Powley (1987) demonstrated that electrical stimulation of the brainstem dorsal vagal nucleus (DMNX), which contains the somata of vagal efferents, increased the release of insulin, glucagon and pancreatic polypeptide from the endocrine pancreas. Whilst this confirms that efferent vagal activity can modulate pancreatic function, it is less clear whether changing ambient glucose levels in the medulla can alter neuronal activity in the dorsal vagal complex.

The body must sense and react to changes in ambient glucose levels in order to maintain blood glucose levels within a narrow range. Glucosensing cells, specialized for this purpose, are found in several tissues. The archetypal glucosensors are the pancreatic β-cells, which secrete insulin in response to a rise in blood glucose levels (Ashcroft & Gribble, 1999). These cells rely on the enzyme glucokinase, a low affinity hexokinase, to provide a quantitative 'translation' of the intracellular glucose concentration into ATP concentration. The concentration of ATP, in turn, governs the activity of the ATP-sensitive K^+ (K_{ATP}) channel, which sets the membrane potential of the β-cell, and hence links cellular metabolism and electrical activity (Trapp & Ashcroft, 1997).

R. H. Balfour and A. M. Kruse Hansen contributed equally to this work.

 DOI: 10.1113/jphysiol.2005.098822

Table 1. Primers for RT-PCR amplification

GenBank no.	Primer	Sequence	Position	Product size (bp)
Glucokinase X53589	Outer forward	ACA TTG TGC GCC GTG CCT GT	1301	951
	Outer reverse	CCT TTC TGG TCC CCT TAG AG	2252	
	Inner forward	CTC CAC ACA CCA CAA ATG CTC C	1646	525
	Inner reverse	CCA CTC GGG TGG AGG TAT ATG AAG	2171	
SUR1 L40624	Outer forward	AAG CTC CTA GAG TAC ACC GA	3861	654
	Outer reverse	CTC TGG GTC CAG GTT GAA TC	4515	
	Inner forward	GTC CGC ATG GAG TAC ATC GGA	3934	493
	Inner reverse	GGC AGC TTG GCG ATG TCA A	4427	

Products span introns to monitor possible genomic contamination. Glucokinase primers recognize both pancreatic and liver isoforms.

In a similar way to β-cells, some central neurones act as glucosensors. Although these were initially reported more than 30 years ago (Oomura *et al.* 1969; Ritter *et al.* 1981), it is only recently that they have received more attention due to their potential role in the regulation of appetite (Rowe *et al.* 1996; Singer & Ritter, 1996; Spanswick *et al.* 1997, 2000; Ritter *et al.* 2000; Levin *et al.* 2001; Miki *et al.* 2001). Some controversy surrounds the relative importance of the different glucosensing CNS sites, but most research has focused on hypothalamic sites such as the ventromedial nucleus and the arcuate nucleus (Ashford *et al.* 1990*a*,*b*; Levin *et al.* 1999; Yang *et al.* 1999; Ritter *et al.* 2000; Miki *et al.* 2001; Yang *et al.* 2004).

Whilst there is growing evidence that hypothalamic glucosensing neurones employ glucokinase to monitor changes in glucose availability, it is still unclear whether this is also true for brainstem neurones (Lynch *et al.* 2000; Maekawa *et al.* 2000; Dunn-Meynell *et al.* 2002). Hypothalamic glucose-excited (GE) neurones increase their electrical activity in response to elevated glucose levels, whereas glucose-inhibited (GI) neurones decrease their activity during hyperglycaemia (Yang *et al.* 1999; Song *et al.* 2001). It has been proposed that hypothalamic GE neurones use a mechanism analogous to β-cells involving both glucokinase and K_{ATP} channels (Dunn-Meynell *et al.* 2002). Although it has been shown by us and others that K_{ATP} channels are present in brainstem neurones of the DMNX (Trapp & Ballanyi, 1995; Karschin *et al.* 1998) and the nucleus tractus solitarii (NTS; Dallaporta *et al.* 2000), conflicting reports exist regarding the presence of glucokinase in the brainstem (Lynch *et al.* 2000; Maekawa *et al.* 2000). The mechanism employed by GI neurones is not yet certain but it has been suggested that they too may rely on glucokinase (Dunn-Meynell *et al.* 2002).

For this study we used non-radioactive *in situ* hybridization (ISH) to assess the distribution of cells expressing glucokinase in the dorsal vagal complex, and then compared this to the electrical responses of neurones in the NTS and DMNX to hypoglycaemia. We were able to demonstrate with ISH and single-cell RT-PCR the presence of glucokinase in a subset of cells of the dorsal vagal complex. This was confirmed by our electrophysiological results, which showed that despite a wide distribution of K_{ATP} channels within this region, only few neurones act as glucosensors. These were located in both NTS and DMNX.

Methods

All animal procedures were performed on 18- to 30-day-old Sprague-Dawley rats of either sex in accordance with the Animals (Scientific Procedures) Act 1986.

Molecular biology

For mRNA isolation, rats were anaesthetized with halothane, decapitated, and the brainstem, pancreas and liver rapidly removed and frozen on liquid nitrogen. The frozen tissue was homogenized and mRNA isolated using a kit (Micro Fast Track, Qiagen, Crawley, UK). Alternatively, for single-cell RT-PCR, the cytoplasm from individual cells was harvested into sterile-filtered pipette solution by suction at the end of a patch-clamp recording. During suction care was taken not to break the gigaseal between electrode and cell membrane.

In both cases, first strand cDNA was synthesized for 1 h at 37°C in reverse transcription buffer containing 5 μM random hexamer primers, 20 mM dithiothreitol, 0.5 mM (each) dNTPs, 20 U ribonuclease inhibitor (Promega, Southampton, UK) and 100 U Superscript II reverse transcriptase (Invitrogen, Paisley, UK). Multiplex PCR amplification (for primers see Table 1) was carried out using a hot start protocol with Taq polymerase in a Perkin Elmer Thermal Cycler 9700 (30 cycles: 30 s at 94°C, 60 s at 55°C, 3 min at 72°C). This was followed by a second PCR amplification using nested primers (Table 1) and 2 μl of the first PCR product as template. PCR samples were analysed by agarose gel electrophoresis and visualized using ethidium bromide. Bands corresponding to glucokinase were detected from

brainstem, liver and pancreas PCR products, but not in any of the controls (Fig. 1). Glucokinase could be detected in a 1 : 1000 dilution of pancreas but not brainstem cDNA. In contrast, SUR1 and Kir6.2 were amplified from dilutions up to 1 : 10000 from brainstem cDNA (Fig. 1). The PCR products were verified by direct sequencing (MWG Biotech AG, London, UK).

As negative controls for single-cell RT-PCR, reactions were routinely performed with H_2O instead of DNA sample, with solution from pipettes that were inserted into the slice without recording from a cell, and with samples that were not reverse transcribed (Fig. 8*D*). For positive controls, PCRs were performed on a 1 : 100 dilution of brainstem cDNA.

Histology

Rats were anaesthetized by intraperitoneal injection of pentabarbitone (Sagatal; 60 mg kg^{-1}) and transcardially perfused with ice-cold heparinized saline followed by ice-cold 4% paraformaldehyde in phosphate buffer (PB). This procedure was selected to (a) maintain good cellular morphology, and (b) inactivate almost instantaneously any enzymes interfering with the mRNA expression pattern. The brain was removed and postfixed with 4% paraformaldehyde at 4°C overnight. Brains were cryoprotected with 30% sucrose in phosphate buffered saline (PBS), and 30 μm coronal brainstem sections were cut using a cryostat.

***In situ* hybridization.** For riboprobe generation, the glucokinase PCR product was subcloned into a suitable vector (TOPO TA Cloning kit; Invitrogen). For SUR1 riboprobes, its coding region was inserted into pcDNA3. Sense and antisense riboprobes were generated by *in vitro* transcription (Riboprobe® *in vitro* Transcription system, Promega) from the linearized vector in the presence of biotin-conjugated UTP (Roche). Subsequently the riboprobes were purified (RNeasy® Mini Kit, Qiagen) and used for ISH.

Cryostat sections were incubated in hybridization solution containing 50% formamide, 10% dextran sulphate, 1 × Denhardt's solution, 4 × sodium citrate buffer (SSC), 250 μg ml^{-1} denatured salmon sperm DNA and 250 μg ml^{-1} tRNA at RT for 30 min and at 37°C for 1 h. Antisense or sense riboprobes (~0.5 ng μl^{-1}) were added and sections were incubated in reaction tubes in a Thermomixer (Eppendorf, Germany) overnight at 55°C. After hybridization sections were washed once at 55°C and twice at 37°C in 4 × SSC with 10 mM sodium thiosulphate (NaTS) added, followed by identical washes in 2 × SSC and 10 mM NaTS and in 0.5 × SSC at 37°C. This was followed by a final wash in 0.1 × SSC at 55°C. Sections were then transferred into Tris-buffered saline (TBS), washed 3 ×, blocked with casein solution (Vector Laboratories Ltd, Peterborough, UK) in TBS for 30 min at RT and incubated overnight at 4°C with avidin-conjugated alkaline phosphatase (Vector Laboratories). After two washes in TBS, slices were rinsed in NMT (0.1 M NaCl and 50 mM $MgCl_2$ in 0.1 M Tris, pH 9.5). Sections were incubated with filtered BCIP/NBT colour substrate (Sigma) and levamisol (250 mg l^{-1}) in the dark at RT. The reaction was quenched by three rinses in 0.1 M Tris/1 mM EDTA, pH 8.5, and one wash with tapwater. Sections were either used for glial fibrillary acidic protein (GFAP) immunofluorescence (see below) or mounted on glass slides and coverslipped with Vectashield (Vector Laboratories).

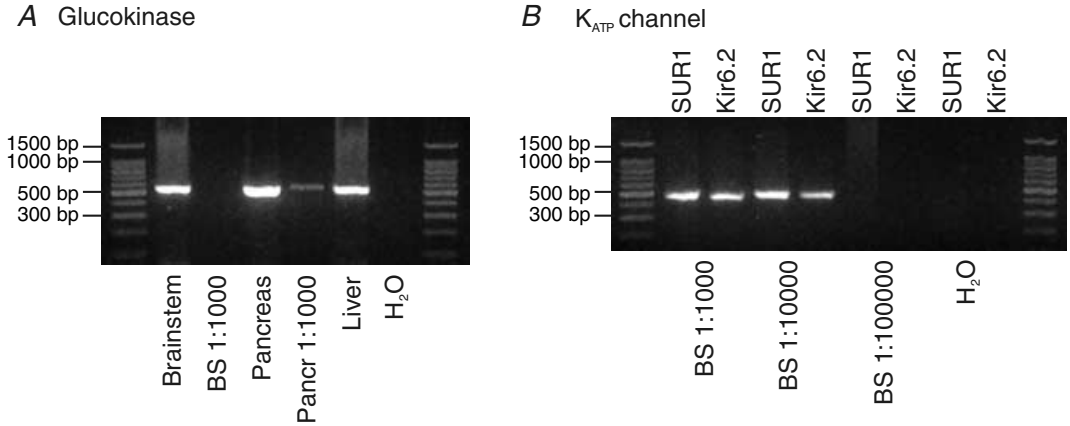

Figure 1. Expression of glucokinase and SUR1 in the dorsal vagal complex
A, 2% agarose gel demonstrating the 525 bp PCR product for glucokinase obtained with the primers specified in Table 1 from cDNA generated from brainstem, pancreas and liver mRNA. BS 1 : 1000: brainstem cDNA diluted 1000 ×; Pancr: pancreas cDNA; H_2O: negative control using deionized water instead of cDNA. *B*, 2% agarose gel demonstrating the sensitivity of primers for K_{ATP} channel subunits SUR1 (493 bp PCR product) and Kir6.2 (478 bp PCR product). Both subunits could be amplified from brainstem cDNA in a 10 000 ×, but not 100 000 ×, dilution.

Table 2. Basic electrical properties of DVN, NNST and glucosensing neurones

	DVN ($n = 88$)	NNST ($n = 51$)	GE ($n = 11$)	GI ($n = 15$)
Input resistance (GΩ)	0.81 ± 0.06	0.98 ± 0.12	0.69 ± 0.09	0.75 ± 0.23
Membrane capacitance (nF)	55 ± 2	$27 \pm 2^{**}$	36 ± 4	50 ± 7
Resting membrane potential (mV)	-54 ± 1	-56 ± 1	-56 ± 2	-58 ± 2
Spontaneous activity (Hz)	2.4 ± 0.3	2.3 ± 0.33	3.5 ± 0.7	2.1 ± 0.6
Afterhyperpolarization amplitude (mV)	22 ± 1	$17 \pm 1^{*}$	n/a	n/a

Statistical significance was tested for DVN against NNST and GE against GI neurones. $^{**}P < 0.01$, $^{*}P < 0.05$.

Negative controls were performed firstly by incubating the slices with sense riboprobes. Secondly, sections were digested with RNase A before hybridization: 30 min in RNase buffer (20 μg ml^{-1} RNase A (Sigma), 500 mM NaCl, 10 mM Tris, 1 mM EDTA pH 8) at 37°C. These sections were washed twice in RNase buffer (minus RNase) then four times in saline before incubation with hybridization solution. Finally, hybridizations were performed at 65°C instead of 55°C. All of these treatments led to an absence of positive staining.

GFAP immunocytochemistry. After completion of the *in situ* hybridization protocol and the final rinse in tapwater, sections were washed three times in PBS and incubated for 30 min in block solution (10% goat serum, 1% BSA, 0.1% Triton X-100 in PBS), followed by overnight incubation with a monoclonal mouse antibody against GFAP conjugated to Cy3 (1 : 500; Sigma) in block solution at RT. After three washes in PBS, slides were mounted and coverslipped with Vectashield.

Electrophysiological studies

Brainstem slices (200 μm) were obtained from rats after anaesthesia (Sagatal; 60 mg kg^{-1}; intraperitoneal) and transcardial perfusion with low Na^+ solution containing (mM): 200 sucrose, 2.5 KCl, 28 $NaHCO_3$, 1.25 NaH_2PO_4, 3 sodium pyruvate, 7 $MgCl_2$, 0.5 $CaCl_2$ and 7 glucose (pH 7.4). After recovery at 34°C for 30 min in a solution containing (mM) 118 NaCl, 3 KCl, 25 $NaHCO_3$, 1.2 NaH_2PO_4, 7 $MgCl_2$, 0.5 $CaCl_2$ and 2.5 glucose (pH 7.4), slices were kept at RT in ACSF of the following composition (mM): 118 NaCl, 3 KCl, 25 $NaHCO_3$, 1.2 NaH_2PO_4 1 $MgCl_2$, 1.5 $CaCl_2$, and 10 glucose (pH 7.4). Hypoglycaemic ACSF was prepared by equimolar replacement of glucose with sucrose. Patch pipettes were pulled from thin-walled borosilicate capillaries (3–6 MΩ; Clark Electromedical Instruments, Pangbourne, UK) with a horizontal puller (Zeitz, Germany). Electrodes were filled with (mM) 120 potassium gluconate, 1 NaCl, 1 $MgCl_2$, 1 $CaCl_2$, 10 Hepes, 10 EGTA, pH 7.2 and varying concentrations of K_2ATP.

Whole-cell recordings were carried out in ACSF at RT. Most drugs were directly added to the ACSF. Tolbutamide and diazoxide were prepared in 0.1 M NaOH as 0.05 M and 0.02 M stock solutions, respectively. TTX was prepared as 1 mM stock solution in citrate buffer. The recording chamber (volume 2 ml) was perfused with ACSF at a rate of 4–5 ml min^{-1}.

Recordings were performed in both voltage clamp and current clamp mode using an EPC-9 amplifier and Pulse/Pulsefit software (Heka Elektronik, Lambrecht, Germany). Currents or membrane potentials were filtered at 1 kHz and digitized at 4 kHz. Membrane resistance was monitored with 500 ms current or voltage pulses every 5 s. Current–voltage (I–V) relationships were obtained either by analysing hyperpolarizing and depolarizing 200 ms voltage or current steps, or by holding the cell at −20 mV for a minimum of 30 s and then applying a voltage ramp from −20 to −120 mV over 700 ms. Compensation for the junction potential (+ 10 mV) was performed offline. Recordings displayed in figures are adjusted for the junction potential.

Data are given as the mean ± 1 S.E.M. Statistical significance was tested using an unpaired Student's t test, unless stated otherwise. P-values of < 0.05 (*) or < 0.01 (**) were taken to indicate that the data were significantly different.

Results

Electrophysiological analysis

Basic properties of neurones in the dorsal vagal complex. Whole-cell recordings were obtained from cells in the dorsal vagal complex. Individual cells were classified as dorsal vagal neurones (DVNs; $n = 108$) or neurones of the nucleus of the solitary tract (NNSTs; $n = 65$) by their localization within the slice and additionally by the fusiform shape of DVNs. Both cell populations had similar basic electrical properties (Table 2), however, DVNs were on average larger and 83% were spontaneously active. In contrast, only 61% of NNSTs were spontaneously active with a significantly smaller afterhyperpolarization than DVNs (Table 2).

Whole-cell recordings were performed with either 0, 1, 2, or 3 mM ATP added to the pipette solution to determine if the amount of ATP supplied via the pipette determines the activity of ATP-sensitive K^+ (K_{ATP}) channels in DVNs and NNSTs. Spontaneous hyperpolarization, or outward

currents that developed upon establishing the whole-cell configuration, was observed in 9% of recordings with ATP-free pipette solution ($n = 56$), in 4% of recordings with 1 mM ATP ($n = 25$), in 3% of recordings with 2 mM ATP ($n = 75$), but in no recordings with 3 mM ATP ($n = 17$). These currents were blocked by the sulphonylurea tolbutamide (100 μM; Fig. 2*A*), confirming their identity as K_{ATP} currents (see also: Trapp *et al.* 1994). Cells showing spontaneous activation of K_{ATP} currents were excluded from the rest of the study.

For the remaining cells ($n = 165$), the pipette ATP concentration had no influence on the mean resting potential, the resting membrane conductance or the percentage of cells showing K_{ATP} current activation in response to metabolic challenges (1 mM cyanide (Fig. 2*B*) or 3 mM azide (Fig. 3*C*)). This is exemplified for DVNs in Table 3. These results suggest that intrinsic energy metabolism rather than pipette ATP concentration determines the intracellular/submembraneous ATP concentration of vagal neurones in whole-cell recordings with series resistance in the range of 8–25 MΩ. Accordingly, the whole-cell configuration appears to be a valid mode for the recording of membrane currents under metabolic challenges such as hypoglycaemia or mitochondrial inhibition by cyanide.

K_{ATP} currents. Pharmacological activation and inhibition of K_{ATP} channels was used to determine the proportion of neurones within the dorsal vagal complex that possess functional K_{ATP} channels. Diazoxide (200 μM) was used as a K_{ATP} channel opener and tolbutamide (100 μM) as an inhibitor. Bath application of tolbutamide had no effect on membrane current or whole-cell conductance ($n = 5$; Fig. 2*C*), whereas diazoxide activated a current with a reversal potential of -83 ± 1 mV ($n = 6$; Fig. 2*C*). Cyanide (1 mM) caused an outward current with a reversal potential of -76 ± 1 mV ($n = 17$; Fig. 2*B*), and azide (3 mM) led to a current with a reversal potential of -75 ± 5 mV ($n = 9$). All three responses were inhibited by tolbutamide (100 μM) with a reversal potential of

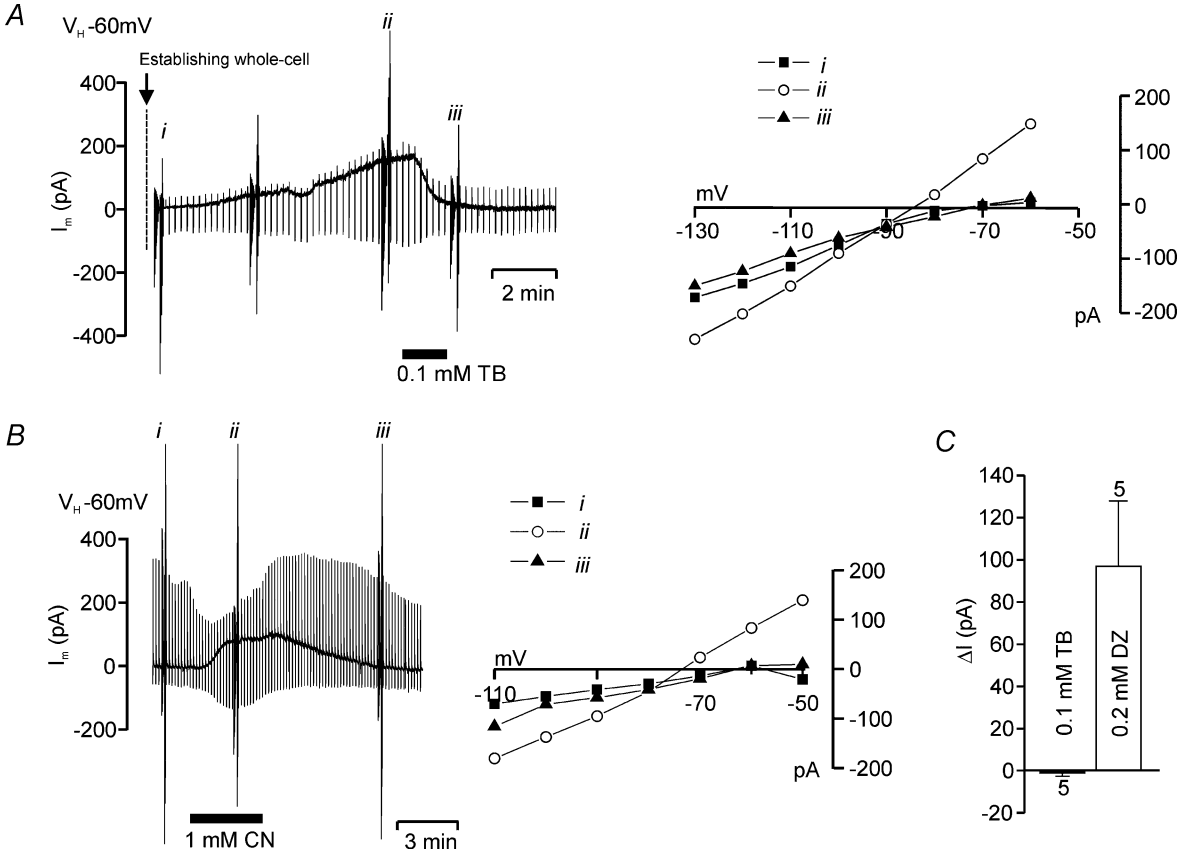

Figure 2. K_{ATP} channels in the dorsal vagal complex
A, left, voltage-clamp recording demonstrating spontaneous outward current triggered by whole-cell configuration (ATP-free pipette solution). Tolbutamide was bath applied as indicated by the black bar. Right, current–voltage relations for time points indicated. *B*, voltage-clamp trace from a DVN. Downward deflections indicate the current response to −40 mV voltage steps of 500 ms duration every 5 s. i, ii and iii indicate current responses to voltage pulses used to generate current–voltage relations shown. *C*, mean change in holding current at −60 mV upon application of 0.1 mM tolbutamide (TB) or 0.2 mM diazoxide (DZ).

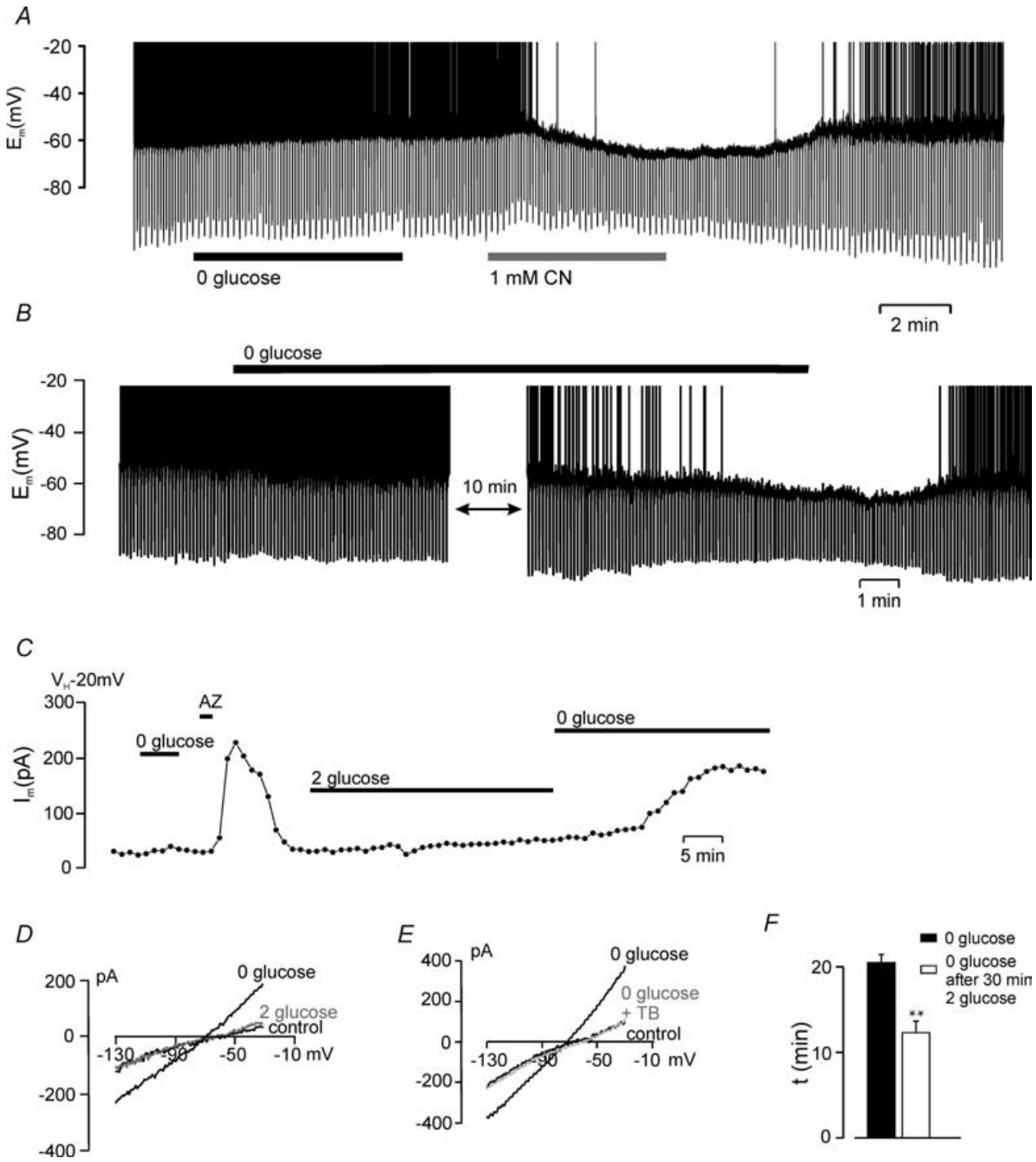

Figure 3. K_{ATP} currents in glucose non-responsive (NR) neurones in response to prolonged hypoglycaemia

A, current-clamp recording from a NR NNST with functional K_{ATP} channels as indicated by the response to cyanide. 0 glucose and 1 mM cyanide (CN) were bath-applied as indicated by the black and grey bars, respectively. Downward deflections of the voltage trace were caused by alternating current pulses of −60 and −80 pA amplitude and 500 ms duration every 5 s. Action potential amplitude is truncated at −20 mV. *B*, prolonged exposure (23 min) of an NR neurone to glucose-free solution as indicated by the black bar led to a reversible hyperpolarization and increase in membrane conductance. Downward deflections represent the voltage response to repetitive 500 ms injections of −60 pA current. *C*, voltage-clamp recording from an NR neurone. 5 min of 0 mM and 30 min of 2 mM glucose had no clear effect on the standing outward current at −20 mV. In contrast, 3 mM sodium azide or prolonged exposure to glucose-free ACSF led to a reversible, pronounced increase in outward current. *D*, current–voltage relations from the recording in *C* at various time points. Prolonged exposure to zero glucose,

Table 3. Basic electrical properties of NR DVN recorded with zero, 1 mM or 2 mM ATP added to the patch-pipette solution

	Zero ATP	1 mM ATP	2 mM ATP
R_m (mV)	-55 ± 3 (11)	-53 ± 2 (7)	-53 ± 1 (19)
Input resistance (GΩ)	0.81 ± 0.09 (23)	0.82 ± 0.11 (17)	0.76 ± 0.09 (19)
Spontaneous activity (Hz)	3.4 ± 0.7 (9)	2.7 ± 0.6 (8)	1.6 ± 0.3 (17)
Membrane capacitance (nF)	53 ± 3 (23)	50 ± 3 (23)	66 ± 5 (19)
% cells with K_{ATP} currents	38	39	43

Values of *n* are given in parentheses.

-89 ± 2 mV ($n = 20$). These recordings demonstrated functional K_{ATP} currents in 56% of NNSTs and 39% of DVNs.

Responses to hypoglycaemia. Slices were kept in ACSF containing 10 mM glucose since storage of slices in ACSF with 5 mM glucose or less led to a noticeable reduction in the numbers of viable cells within the dorsal vagal complex over the typical storage period of 5 h (S. Trapp, unpublished observation). Hypoglycaemic challenges were induced by switching the superfused ACSF from 10 mM to 2 mM or 0 mM glucose (under equiosmolar substitution with sucrose). Before testing for glucosensing properties, neurones were recorded for a minimum of 5 min after establishing the whole-cell configuration to ensure the absence of spontaneous activation of K_{ATP} channels. A total of 123 neurones (DVNs + NNSTs) were tested for their response to transient hypoglycaemia.

Non-responsive (NR) neurones. Upon exposure to hypoglycaemia, the majority (97 out of 123) of cells showed no alteration of the resting potential within 5–10 min of exposure (Fig. 3*A*). We refer to these cells as 'non-responsive' (NR) neurones by way of analogy to the classification used in studies of hypothalamic glucose sensors (Song *et al.* 2001). Twelve NR cells were further tested for their response to prolonged hypoglycaemia. Five NR cells were exposed to 0 mM glucose for up to 40 min and four of these hyperpolarized after 21 ± 1 min (Fig. 3*B*). The underlying outward current was abolished by 100 μM tolbutamide (Fig. 3*E*). An additional seven NR DVNs were exposed to 2 mM glucose for 30 min. None of these responded with a significant change in membrane potential or current (Fig. 3*C* and *D*). Subsequently, four of these neurones were exposed to 0 mM glucose and after a delay of 12 ± 1 min three of these hyperpolarized or developed an outward current (reversal potential -69 ± 2 mV; Fig. 3*C* and *F*).

Glucose-excited (GE) neurones. A small proportion of cells (11 out of 123) hyperpolarized by 14 ± 2 mV within 53 ± 7 s of glucose removal from the bath perfusate (Fig. 4). This hyperpolarization was reversible upon reapplication of glucose (10 mM) or the K_{ATP} channel inhibitor tolbutamide (100 μM; Fig. 4*A* and *C*) and persisted in the presence of 0.5 μM TTX (Fig. 4*C*). The underlying hypoglycaemia-induced current reversed at -79 ± 3 mV ($n = 7$). An identical response was also evoked by application of 2.5 mM 2-deoxyglucose, a non-metabolisable glucose analogue, in the presence of 10 mM glucose ($n = 2$; Fig. 4*B*). 2-Deoxyglucose at 2.5 mM had no effect on membrane potential or whole-cell conductance of NR cells ($n = 8$).

These glucose-excited (GE) cells were found within both the DMNX and the NTS, and 5 out of 8 GE cells recorded under current clamp conditions fired spontaneous action potentials at a frequency of 3.5 ± 0.7 Hz. Their resting potential, membrane resistance and capacitance were not significantly different from those of glucose non-responsive (NR) neurones (Table 2). Additionally, the amplitude of the afterhyperpolarization of action potentials evoked by depolarizing current injection varied widely between individual GE cells as shown in Fig. 4*D*.

Glucose-inhibited (GI) neurones. Fifteen out of 123 cells depolarized or developed an inward current within 155 ± 31 s of glucose removal from the bath perfusate (Fig. 5, Table 2). Eight of these cells were recorded in current clamp with a mean resting potential of -58 ± 2 mV. Two of these cells were electrically silent under control conditions, and the six remaining cells fired action potentials in the range of 0.3–4.7 Hz (Fig. 5*A* and *B*). The hypoglycaemia-induced depolarization was accompanied by either initiation of action potential firing in cells that were previously quiescent in 10 mM glucose, or a significant ($P < 0.01$, paired *t* test) increase of action potential firing frequency in spontaneously active

but not 2 mM glucose evoked a current with a reversal potential near E_K that is abolished by 0.1 mM tolbutamide (*E*). *F*, mean time to onset of the hypoglycaemia-induced current with and without preincubation in 2 mM glucose. TB: tolbutamide; CN: sodium cyanide; AZ: sodium azide. $^{**}P < 0.01$ unpaired *t* test.

neurones (Fig. 5). The depolarization was progressive and in most cases (6 of 8) irreversible upon reperfusion with glucose. Another seven of these neurones were recorded in voltage clamp. Glucose removal elicited an inward current of -71 ± 20 pA at a holding potential of -60 mV.

We refer to these cells as glucose-inhibited (GI) in analogy to hypothalamic neurones that depolarize in response to reduced glucose availability (Song *et al.* 2001). However, in contrast to hypothalamic GI neurones, these neurones were mostly spontaneously active at resting (5–10 mM) glucose concentrations. Furthermore, the GI cells described in the ventromedial hypothalamus and arcuate nucleus have been proposed to utilize a Cl^- channel to generate their response to hypoglycaemia. In contrast, analysis of current–voltage relations ($n = 12$) of the brainstem GI cells revealed that they fall into three groups. Two cells reduced a conductance with a reversal potential of -95 ± 5 mV near the K^+ equilibrium potential upon glucose removal. In the remaining cells conductance increased under hypoglycaemia with a reversal potential of either -40 ± 3 mV ($n = 5$) or -6 ± 5 mV ($n = 5$; Fig. 5*C–E*). Additionally, recordings were performed in the presence of 0.5 μM TTX to ascertain if the observed responses were intrinsic to the recorded neurones. Glucose removal evoked a depolarization and an increase in whole-cell conductance in one cell (reversal potential -43 mV), and a decrease of conductance with a reversal potential near E_K in two cells.

In situ hybridization

The results presented so far indicate that the presence of K_{ATP} currents is not a reliable indicator for glucosensing properties of a cell. K_{ATP} currents were found in a proportion of NR cells and were not involved in the response of GI cells. Consequently, we next investigated whether glucokinase, an enzyme essential for β-cell glucosensing (Sakura *et al.* 1998), is present in vagal neurones. We used biotin-labelled riboprobes for glucokinase (GLK) and the K_{ATP} channel subunit SUR1 to assess their expression pattern within the dorsal vagal complex in cryostat sections from perfuse-fixed rats

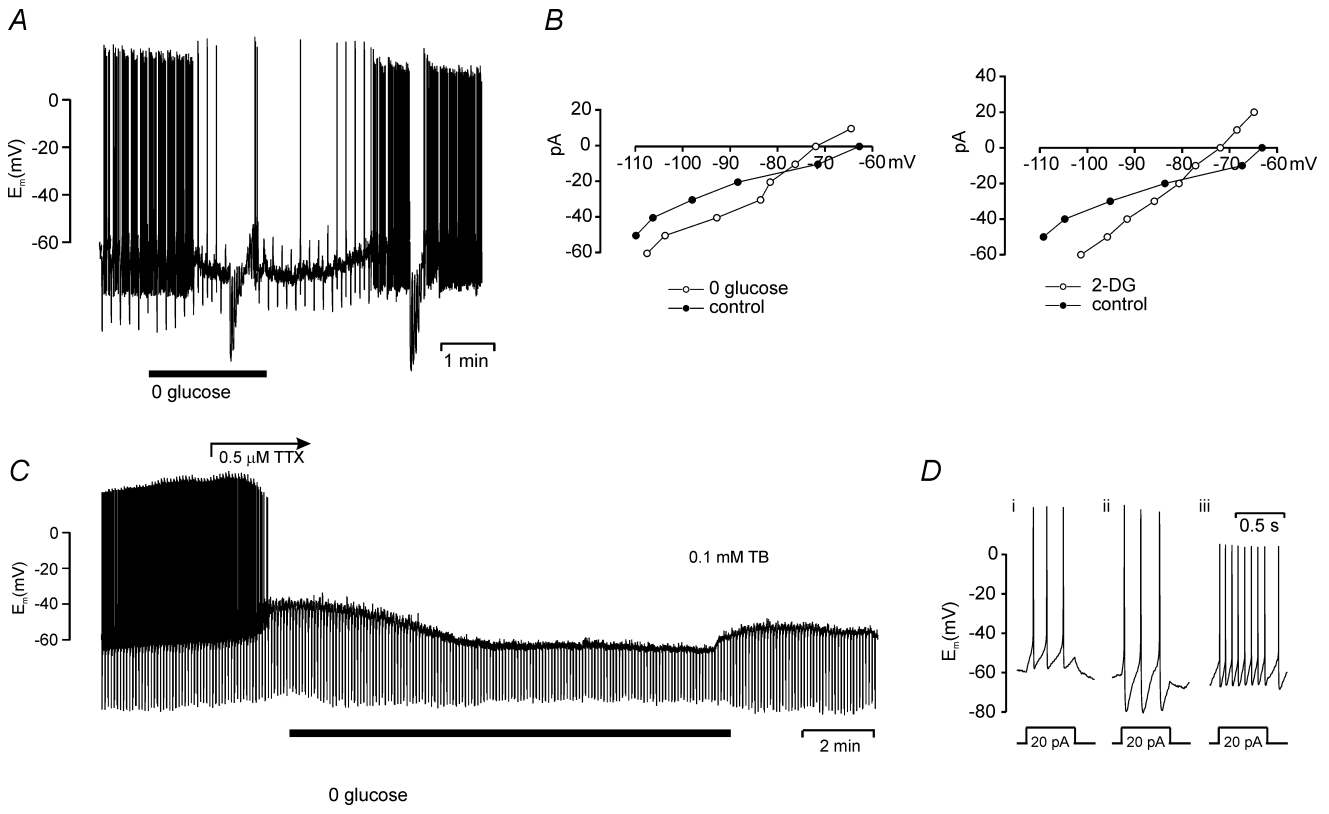

Figure 4. Glucose-excited (GE) neurones in the dorsal vagal complex
Current clamp recordings from GE neurones. *A*, fast and reversible hyperpolarization of a DVN upon glucose removal. *B*, whole-cell current–voltage relations from a DVN in the presence of 10 mM (control) or 0 mM glucose or 2-deoxyglucose (2-DG). The differential current (hypoglycaemia-induced) reversed close to E_K. *C*, recording from an NNST demonstrating that the hypoglycaemia-induced hyperpolarization persisted in 0.5 μM tetrodotoxin (TTX) and was inhibited by tolbutamide (TB). *D*, large variations in amplitude of afterhyperpolarization were observed between different GE cells (i, ii, iii represent different cells recorded).

to retain optimal morphology. Differential interference contrast (DIC) optics were used under high magnification to visualize unstained (GLK- or SUR1-negative) cells.

Hybridization with GLK-antisense riboprobes revealed relatively widespread expression at low levels throughout the brainstem. No staining was observed after hybridization with GLK-sense riboprobes (see supplemental material). Analysis of the dorsal vagal complex demonstrated GLK-positive cells in the DMNX and NTS (Fig. 6*A*). In both of these nuclei GLK was

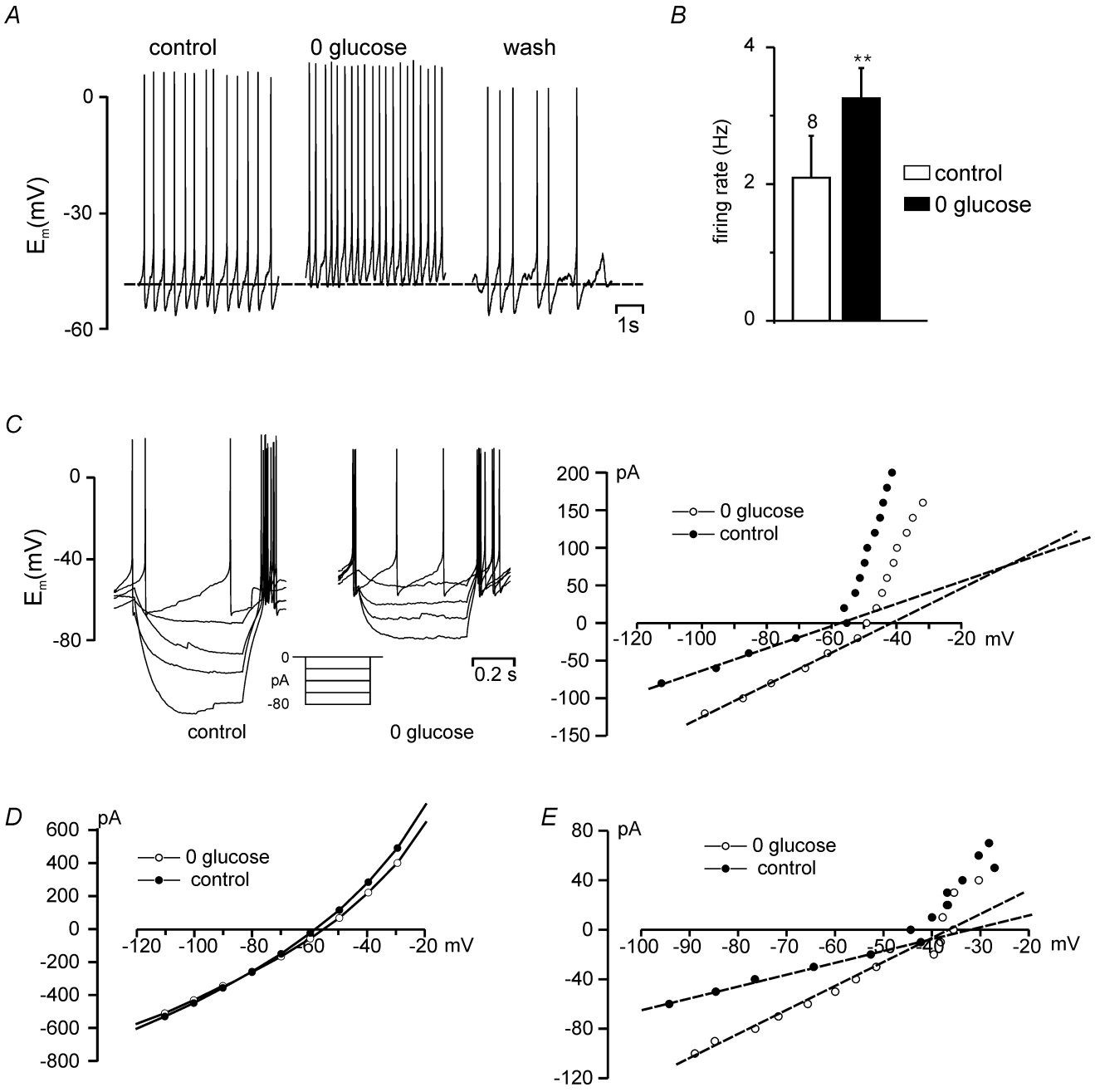

Figure 5. Glucose-inhibited (GI) neurones in the dorsal vagal complex
A, current clamp recording from a GI neurone before, during and after exposure to glucose-free ACSF. No holding current and no current pulses were applied. *B*, mean data from 8 GI cells recorded as in *A*. $^{**}P < 0.01$, paired *t* test. *C–E*, current–voltage relations from 3 GI cells recorded in 10 and 0 mM glucose. In response to glucose removal, cells either increased conductance (reversal potential: ∼0 mV (*C*) or ∼−40 mV (*E*)) or decreased conductance (reversal potential ∼−90 mV (*D*)). Reversal potentials were obtained by extrapolating the linear part of the *I–V* relation (to avoid contributions by voltage-gated channels).

expressed in a considerably smaller number of cells than the K_{ATP} channel subunit SUR1 (Fig. 6*B*). The staining for both GLK and SUR1 was cytoplasmic with the nucleus being clearly spared.

Analysis of the cellular expression pattern within the DMNX and the NTS using DIC optics revealed that only a small subpopulation of cells was positive for GLK (Fig. 6*C* and *E*). GLK-positive cells in both NTS and DMNX were scattered over the rostro-caudal extent of the region examined (equivalent to Bregma −12.80 mm to Bregma −14.60 mm in adult rats; Paxinos & Watson, 1998). Furthermore, within individual sections, there were no apparent differences between medial and lateral or between dorsal and ventral areas of the DMNX and NTS. These results were in good agreement with the electrophysiological findings (i.e. a small percentage of scattered positive cells within the dorsal vagal complex). Also consistent with the electrophysiological results was the observation that a much larger proportion of cells expressed the K_{ATP} channel subunit SUR1 (Fig. 6*B*, *D* and *F*). Strong cellular staining for SUR1 mRNA was found in both the DMNX and the NTS, in agreement with previous studies using radioactive oligonucleotide DNA probes (Karschin *et al.* 1997).

Finally, the possibility that glucokinase is expressed in glial cells, specifically in astrocytes, was explored by a colabelling protocol for GLK *in situ* hybridization and glial acid fibrillary protein (GFAP) immunofluorescence. In the DMNX and the NTS glucokinase mRNA and the glial marker GFAP were not colocalized to the same cells (Fig. 7). This suggested that glucokinase is not expressed by GFAP-positive glial cells.

Single-cell RT-PCR analysis

The results presented so far have demonstrated expression of SUR1 and glucokinase in the dorsal vagal complex and verified that GE cells possess functional K_{ATP} channels, but indicate that this alone is not sufficient to determine a glucosensing phenotype (since some NR cells also showed K_{ATP} currents). Consequently, we tested whether expression of glucokinase in individual cells correlates with

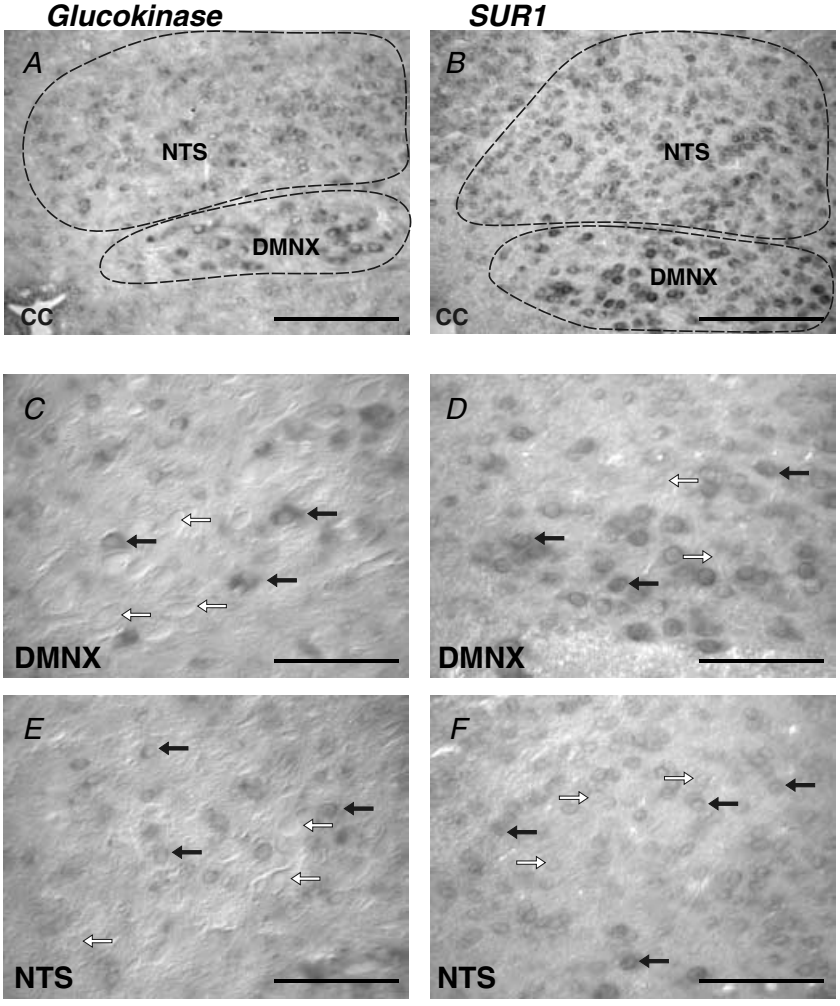

Figure 6. Photomicrographs showing the localization of glucokinase and SUR1 within the dorsal vagal complex
Glucokinase (GLK) mRNA detection by *in situ* hybridization in the dorsal vagal nucleus (DMNX; *A* and *C*) and nucleus tractus solitarius (NTS; *A* and *E*), GLK-positive cells (examples indicated by black arrows) showed cytosolic staining with the nucleus spared. Differential interference contrast (DIC) optics (*C* and *E*) allowed visualization of unstained (GLK-negative) cells (examples indicated by white arrows). CC, central canal. *In situ* hybridization for SUR1 within the DMNX (*B* and *D*) and NTS (*B* and *F*). SUR1-positive cells showed cytosolic staining with the nucleus spared (examples indicated by black arrows. White arrows: negative cells). *A* and *B* bright field optics, *C–F* bright field with DIC. Scale bars: *A* and *B*, 100 μm; *C–F*, 50 μm.

their function as glucosensors. Membrane potentials or currents of 47 neurones were recorded in the whole-cell mode and their glucosensing properties explored by exposure to glucose-free solution. According to their response they were classified as GE, GI or NR, as described above. Subsequently, the cytoplasm of these cells was harvested and its mRNA subjected to reverse transcription. The resulting cDNA was then used as template in a nested PCR protocol with primers as listed in Table 1. Figure 8*A* demonstrates the presence of glucokinase mRNA in a GE dorsal vagal neurone and its absence in a NR neurone. Figure 8*C* shows glucokinase expression in a neurone that depolarized and started firing action potentials during glucose deprivation (GI cell). Glucokinase was not found in any NR cells ($n = 38$), but in all GI cells tested ($n = 5$) and in 3 of 4 GE cells. In contrast, SUR1 was expressed in 17 of 38 NR neurones, 3 of 4 GE cells and in one GI cell (Table 4, Fig. 8*B*).

Discussion

This study provides the first analysis of the defining molecular and electrical mechanisms utilized by glucosensing cells in the dorsal vagal complex of the brainstem. These cells responded to a severe hypoglycaemic challenge considerably faster than other dorsal vagal neurones (Ballanyi *et al.* 1996), and like in pancreatic β-cells, glucokinase expression seems to be of critical importance for the glucosensing phenotype.

Glucose in slices

This study and previous work (Trapp & Ballanyi, 1995; Ballanyi *et al.* 1996; Ballanyi & Kulik, 1998; Müller *et al.* 2002) have demonstrated that a considerable proportion of DVN express K_{ATP} channels and that mitochondrial inhibition causes a hyperpolarization that silences these tonically active cells. Prolonged exposure of these neurones to glucose-free solution (20–30 min) also leads to K_{ATP} channel-mediated hyperpolarization (Ballanyi *et al.* 1996). However, it is important to note that this response would be expected of any cell expressing K_{ATP} channels during severe energy deprivation, and hence does not indicate glucosensing *per se*. The present study was therefore designed to distinguish those cells that merely respond with K_{ATP} currents to severe energy depletion from the true glucosensing cells by identifying neurones that respond to glucose removal in a similar way to pancreatic β-cells (i.e. respond to minor changes in glucose concentration or respond rapidly to acute challenges).

The interstitial glucose concentration in the VMH of fed rats has been determined by microdialysis as ~1.4 mM (De Vries *et al.* 2003). This is considerably lower than that routinely used for (and tolerated by) *in vitro* slice preparations. We observed that storage of brainstem slices at less than 5 mM glucose for several hours led to a noticable loss of cells in the dorsal vagal complex. *In vivo* the microcirculation supplies glucose to the vicinity of every cell, whereas in slices diffusion from the bath solution is the only means of supplying neurones with glucose. With insulin-induced episodes of hypoglycaemia, VMH glucose levels *in vivo* fall rapidly below 0.5 mM (de Vries *et al.* 2003) and cells appear to respond to relatively small alterations of glucose levels. In slices, however, hypoglycaemia is only achieved by the combination of glucose usage and diffusion of glucose out of the slice. Therefore considerably slower responses would be expected *in vitro* than *in vivo*. Our results suggest that NR cells obtain sufficient ATP from 2 mM extracellular glucose to sustain their function and to keep K_{ATP} channels closed. The observation that the development of K_{ATP} currents in response to zero glucose was significantly faster after preincubation in 2 mM glucose, as compared to 10 mM glucose, might indicate that removal of glucose from the slice is relatively slow. We would suggest that this difference of almost 10 min in the

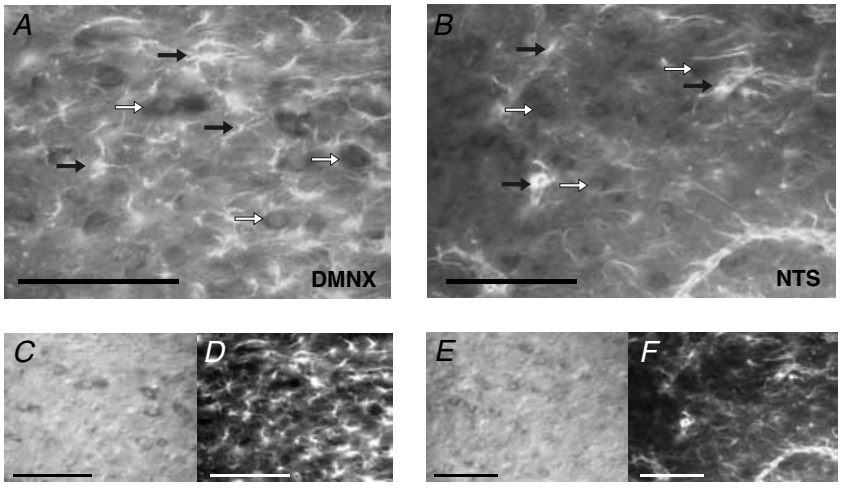

Figure 7. Photomicrographs demonstrating the lack of colocalization of GFAP and glucokinase in the dorsal vagal complex
Glucokinase mRNA (detected by *in situ* hybridization, indicated with white arrows) was not colocalized with GFAP immunoreactivity (indicated by black arrows, showing the characteristic star-like appearance of astrocytes) in the dorsal vagal nucleus (*A*) or in the nucleus tractus solitarii (*B*). *A* and *B* are composites of the glucokinase signal observed under bright field optics (*C* and *D*) and the GFAP fluorescence (*E* and *F*). Scale bars: 100 μm.

Table 4. Expression of mRNA for glucokinase and SUR1 in different cell types

	GI	GE	NR
Number of cells	5	4	38
GLK-positive	5	3	0
SUR1-positive	1	3	17

latency of the K_{ATP} response reflects a quicker drop in slice glucose levels from 2 mM than from 10 mM glucose.

Because of the potentially slow washout of glucose from slices, we decided to look for fast responses to glucose removal from the bath solution, rather than a response to a small reduction in ACSF glucose concentration, to define glucosensing cells. Indeed, we found that approximately 10% of neurones in the dorsal vagal complex hyperpolarized within 1 min of glucose removal. This is likely to reflect a response to the modest initial decrease in glucose levels within the slice, since our results from NR neurones suggest that slice glucose levels would not drop to 0 mM within this time.

Interestingly, the latency from perfusion of glucose-free solution to the electrical response was longer for GI cells than for GE cells. A similar difference has recently been reported for hypothalamic GE and GI neurones (Kang *et al.* 2004). This might indicate that ATP levels have to fall further in GI cells to elicit a response, suggesting that the safety margin between generating a signal and severely compromising cellular function is narrower in GI than in GE cells. In support of this hypothesis we found that less GI cells than GE cells recovered from a hypoglycaemic challenge.

We found that brainstem GI neurones fell into three categories in their response to hypoglycaemia: one that was likely to close K^+ channels, one that opened a conductance with a reversal potential of 0 mV, and one that increased a conductance with a reversal at −40 mV. This is different from hypothalamic GI cells, where only closure of a Cl^- channel has been proposed to underlie the depolarization (Song *et al.* 2001). It will be an interesting challenge to further characterize the underlying metabolically sensitive conductances in these brainstem GI neurones.

ATP concentration in patch pipette

Our results suggest that ATP supplied via the patch pipette in whole-cell recordings of vagal neurones in brainstem slices does not replace metabolically produced ATP as the major determinant of K_{ATP} channel activity. However, omission of ATP from the pipette solution can act as a

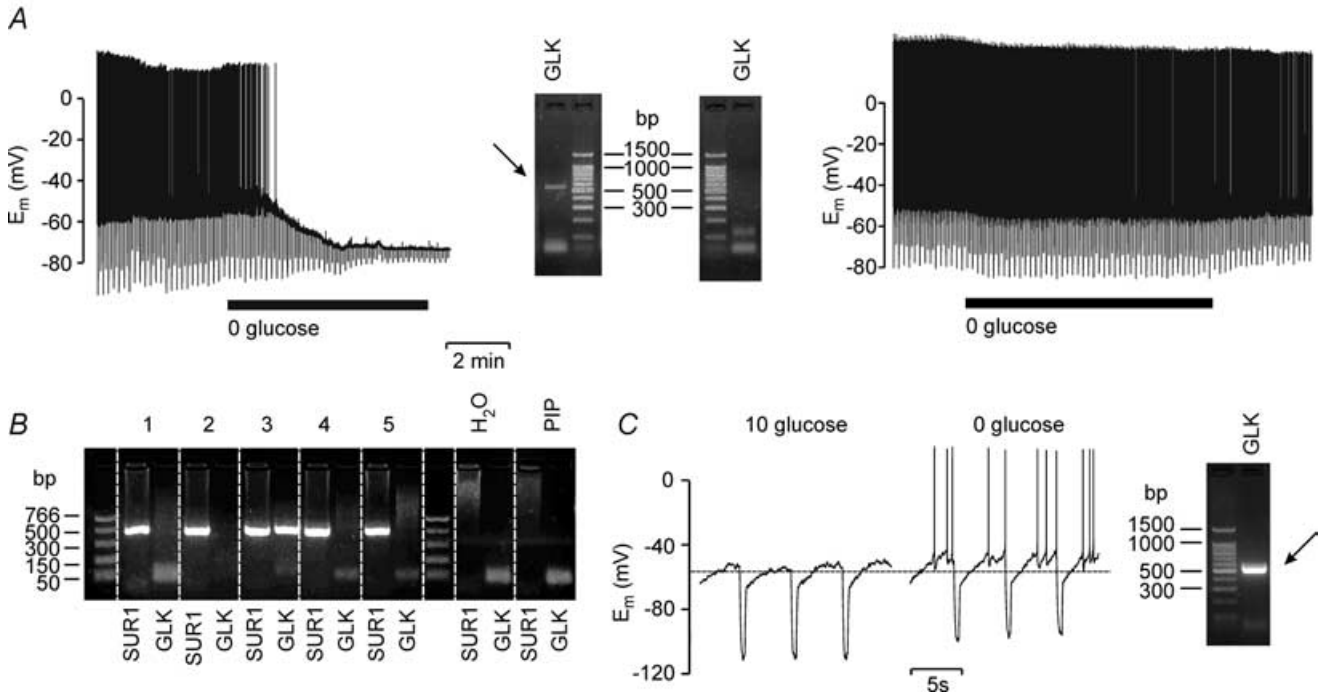

Figure 8. Single-cell RT-PCR analysis of glucokinase expression in the dorsal vagal complex
A, left, GE cell that hyperpolarized in response to glucose removal and expressed glucokinase (525 bp product, arrow). Right, NR cell that lacked response to removal of glucose and lacked glucokinase expression. *B*, typical single-cell RT-PCR analysis for glucokinase (GLK) and SUR1 of 5 neurones. 1, 2, 4, 5: NR neurones; 3: GE neurone. Controls: PIP, pipette solution without cytoplasm extracted from cell. H_2O, no cDNA. *C*, current clamp recording from a GI neurone positive for GLK mRNA.

drain for metabolically produced ATP and thus lead to spontaneous opening of K_{ATP} channels. This indicates that, in contrast to the situation in isolated pancreatic β-cells, the whole-cell mode is indeed a viable recording configuration to assess metabolic sensitivity of neurones in brain slices. This observation is in line with reports on the response of hypothalamic neurones to variations in glucose availability (Spanswick *et al.* 1997; Song *et al.* 2001) and similar to that by Müller *et al.* (2002) in dorsal vagal neurones, who concluded that vagal K_{ATP} channels are metabolically sensitive, but that ATP levels are not the relevant signal. However, our finding that omission of ATP can have an effect on K_{ATP} channel activity in these cells might indicate that perfusion with ATP from the pipette simply cannot significantly alter the ATP levels set by endogenous metabolism. This may be due to cell morphology and location of K_{ATP} channels on dendrites, or alternatively the existence of K_{ATP} channels (and possibly glucose transporters) in microdomains in close proximity to mitochondria.

Histological results

ISH suggests that a small subpopulation of neurones in the lower brainstem express glucokinase. Our electrophysiological recordings indicate that very few cells act as true glucosensors. This might explain why they have not been detected in a few previous studies (Ballanyi *et al.* 1996; Lynch *et al.* 2000). ISH produced cytosolic staining indicating the morphology of positive cell bodies. DIC images from these slices also confirmed that the use of perfuse-fixed tissue for the ISH study maintained cell morphology. Glucokinase-positive cell bodies did not express GFAP, were clearly larger than astrocytes (indicated by astrocytic GFAP expression) and had a similar morphology to the neurones observed in our electrophysiological studies. This suggests that glucokinase is located in the neurones, but not glial cells, of the dorsal vagal complex. This view is further supported by single-cell RT-PCR detection of glucokinase in electrophysiologically confirmed GE and GI neurones in the current study.

These results do not preclude the possibility that glial cells act as glucosensors in a glucokinase-independent fashion and that they modulate the activity of other vagal neurones. However, the release of lactate by glial cells during hypoglycaemia (Deitmer, 2001; Gruetter, 2003) and its uptake by glucosensing neurones would short-circuit any impact of glucokinase on neuronal metabolism, as lactate enters the metabolic pathway downstream of glucose. Consequently, the availability of lactate to glucokinase-dependent glucosensors would abolish their glucosensing properties. In fact, it has been shown that lactate injection into the ventromedial hypothalamus during systemic hypoglycaemia suppressed counter-regulatory responses (Borg *et al.* 2003). Consequently, exposure of glucosensing neurones to glial lactate during hypoglycaemic episodes would appear to be counterproductive.

Single-cell RT-PCR

Both our electrophysiological recordings and the single-cell RT-PCR demonstrated that K_{ATP} channels are required for the function of GE glucosensors, but that their expression is not limited to these cells. The observation that one GE cell seemingly failed to express SUR1 could indicate that some GE cells utilize the SUR2B subunit, as previously identified in substantia nigra neurones (Liss *et al.* 1999). However, the fact that the same GE neurone also failed to express glucokinase might instead suggest that an insufficient amount of mRNA was harvested from that particular cell.

In contrast to the findings for SUR1, the single-cell RT-PCR results for glucokinase suggest a tight link between glucokinase expression and glucosensing properties. Glucokinase mRNA was not detected in any NR cell and in all but one glucosensing cell. Whilst our study confirmed the importance of glucokinase for neuronal glucosensing in the brainstem, a recent study in the hypothalamus using similar techniques failed to produce this tight link, although it did produce a similar trend: Kang *et al.* (2004) found glucokinase mRNA in 8% of NR cells, 43% of GI cells and 64% of GE cells.

Comparison between histological, *in vivo* and *in vitro* results

Our ISH and single-cell RT-PCR results suggest that expression of glucokinase in the brainstem is much more limited than expression of the K_{ATP} channel subunit SUR1. This is in agreement with our electrophysiological data that showed K_{ATP} currents in around 50% of neurones in the dorsal vagal complex and a glucosensing phenotype in approximately 17%. In contrast, an *in vivo* study has suggested that up to 70% of NTS neurones respond to changes in systemic glucose concentration (Yettefti *et al.* 1997). However, this would probably include the response of vagal afferents to peripheral glucosensors as well as projections from hypothalamic glucosensors. In contrast, the persistence of glucose responses in the presence of TTX in the present study, coupled with the tight correlation between a glucosensing phenotype and cellular expression of glucokinase, indicates that we identified neurones that are intrinsic glucosensors only. This could explain why the present results suggest a much lower percentage of glucosensing neurones within the dorsal vagal complex. Whilst is seems feasible that the trauma and metabolic stress during the preparation of *in vitro* brainstem slices could lead to the loss of a percentage of glucosensing cells, our *in situ* hybridization study, which

was performed on the brainstem of perfused-fixed rats, also failed to suggest expression of glucokinase in a large proportion of neurones within the dorsal vagal complex, as suggested by Yettefti *et al.* (1997). However, this argument is based on the assumption that glucokinase is required for glucosensing (Dunn-Meynell *et al.* (2002) and this study), and recently a novel glucosensing mechanism that does not involve glucokinase has been discovered in L-cells of the gut (Gribble *et al.* 2003). Whilst our sc-RT PCR results argue that glucokinase expression and a glucosensing phenotype are linked, the relatively small sample size (38 non-responsive and 9 glucosensing cells) leaves the possibility that some neuronal glucosensors employ the same mechanism as the L-cells.

It is also noteworthy that *in vitro* brainstem slice recordings by Ferreira *et al.* (2001) demonstrated an outward current in response to hyperglycaemia in 38% of gastric-projecting DVN. This current was strongly suppressed by picrotoxin or TTX, suggesting the involvement of GABAergic transmission further upstream, rather than direct glucose effects on gastric-projecting DVN. This lack of a direct effect of glucose as compared to the present study might indicate that gastric-projecting DVN do not act as glucosensors. This conclusion is further supported by the lack of effect on gastric motility and tone of microinjection of glucose into rat DMNX *in vivo* in the same study (Ferreira *et al.* 2001).

Ferreira *et al.* (2001) noticed that K_{ATP} channel blockers were able to mimic the effects of hyperglycaemia on synaptic currents evoked by NTS stimulation. This might indicate the involvement of the NTS GE neurones identified in the present study. Interestingly, these results suggest that K_{ATP} channels of NTS glucosensing neurones are open under resting recording conditions (5 mM glucose; 35°C) in the Ferreira study, because the K_{ATP} channel antagonist glibenclamide mimicked the effects of hyperglycaemia, whereas under our resting conditions (10 mM glucose, 22°C) K_{ATP} channels are inhibited, as demonstrated by the lack of effect of tolbutamide (Fig. 2*C*).

Potential physiological role of NTS and DMNX glucosensors

The results from *in situ* hybridization for glucokinase suggest that glucosensors are scattered throughout both the NTS and the DMNX. This idea is also supported by the electrophysiological results which identified both GE and GI neurones in both nuclei. Our results suggest that central glucosensors are present in both afferent and efferent pathways of the vagal system. We would speculate that those glucosensors in the NTS modulate satiety signals received from visceral chemo- and mechanoreceptors. It is conceivable that some of the NTS glucosensors participate in ascending pathways involved in the regulation of food intake, as microinjection of glucose antimetabolites into various brainstem sites in conscious rats has suggested (Ritter *et al.* 2000). Others might project to the DMNX and are likely to be responsible for the *in vivo* inhibition of gastric motility and tone observed upon glucose microinjection into the NTS (Ferreira *et al.* 2001). In contrast, glucosensing DVN are unlikely to be involved in the modulation of gastric tone and motility (Ferreira *et al.* 2001) but might regulate vagal discharges to the endocrine pancreas, thereby modulating release of insulin or glucagon and ultimately blood glucose levels (Laughton & Powley, 1987; Berthoud *et al.* 1990).

Conclusion

In summary, we have demonstrated that glucosensing neurones employing glucokinase are present in the dorsal vagal complex of the brainstem, confirming that this site is likely to play a role in neuronal/central regulation of glucose homeostasis. We have further shown that K_{ATP} channels are abundant in vagal neurones; however, although these channels play a role in the hypoglycaemic response of glucose-excited neurones, their presence alone is not indicative of glucose sensitivity. Our results also suggest that glucosensing in the dorsal vagal complex is achieved via a direct neuronal response. The finding that DVN in addition to NNST act as glucosensors, together with the observation from Ritter *et al.* (2000) that counter-regulatory blood glucose responses can be elicited by 5-thio-D-glucose injection into the DVN (but not into hypothalamic sites), might indicate that these DVNs are primary sensors and effectors for central nervous modulation of insulin release. It will be interesting to see whether retrograde tracing studies from the pancreas support this hypothesis and if the cephalic phase of insulin release is suppressed by brain hypoglycaemia.

References

Ashcroft FM & Gribble FM (1999). ATP-sensitive K^+ channels and insulin secretion: their role in health and disease. *Diabetologia* **42**, 903–919.

Ashford ML, Boden PR & Treherne JM (1990*a*). Glucose-induced excitation of hypothalamic neurones is mediated by ATP-sensitive K^+ channels. *Pflugers Arch* **415**, 479–483.

Ashford ML, Boden PR & Treherne JM (1990*b*). Tolbutamide excites rat glucoreceptive ventromedial hypothalamic neurones by indirect inhibition of ATP-K^+ channels. *Br J Pharmacol* **101**, 531–540.

Ballanyi K, Doutheil J & Brockhaus J (1996). Membrane potentials and microenvironment of rat dorsal vagal cells in vitro during energy depletion. *J Physiol* **495**, 769–784.

Ballanyi K & Kulik A (1998). Intracellular Ca^{2+} during metabolic activation of K_{ATP} channels in spontaneously active dorsal vagal neurons in medullary slices. *Eur J Neurosci* **10**, 2574–2585.

Bernard C (1855). *Lecons de Physiologie Experimentale Appliquee a la Medecine: Faites Au College de France*. J.B. Bailliere et fils, Paris.

Berthoud HR, Fox EA & Powley TL (1990). Localisation of vagal preganglionics that stimulate insulin and glucagon secretion. *Am J Physiol* **258**, R160–R168.

Berthoud HR & Powley TL (1990). Identification of vagal preganglionics that mediate cephalic phase insulin response. *Am J Physiol* **258**, R523–R530.

Borg MA, Tamborlane WV, Shulman GI & Sherwin RS (2003). Local lactate perfusion of the ventromedial hypothalamus suppresses hypoglycemic counterregulation. *Diabetes* **52**, 663–666.

Dallaporta M, Perrin J & Orsini JC (2000). Involvement of adenosine triphosphate-sensitive K^+ channels in glucose-sensing in the rat solitary tract nucleus. *Neurosci Lett* **278**, 77–80.

De Vries MG, Arseneau LM, Lawson ME & Beverly JL (2003). Extracellular glucose in rat ventromedial hypothalamus during acute and recurrent hypoglycemia. *Diabetes* **52**, 2767–2773.

Deitmer JW (2001). Strategies for metabolic exchange between glial cells and neurons. *Respir Physiol* **129**, 71–81.

Dunn-Meynell AA, Routh VH, Kang L, Gaspers L & Levin BE (2002). Glucokinase is the likely mediator of glucosensing in both glucose-excited and glucose-inhibited central neurons. *Diabetes* **51**, 2056–2065.

Ferreira M Jr, Browning KN, Sahibzada N, Verbalis JG, Gillis RA & Travagli RA (2001). Glucose effects on gastric motility and tone evoked from the rat dorsal vagal complex. *J Physiol* **536**, 141–152.

Gribble FM, Williams L, Simpson AK & Reimann F (2003). A novel glucose-sensing mechanism contributing to glucagon-like peptide-1 secretion from the GLUTag cell line. *Diabetes* **52**, 1147–1154.

Gruetter R (2003). Glycogen: the forgotten cerebral energy store. *J Neurosci Res* **74**, 179–183.

Kang L, Routh VH, Kuzhikandathil EV, Gaspers LD & Levin BE (2004). Physiological and molecular characteristics of rat hypothalamic ventromedial nucleus glucosensing neurons. *Diabetes* **53**, 549–559.

Karschin A, Brockhaus J & Ballanyi K (1998). K_{ATP} channel formation by the sulphonylurea receptors SUR1 with Kir6.2 subunits in rat dorsal vagal neurons in situ. *J Physiol* **509**, 339–346.

Karschin C, Ecke C, Ashcroft FM & Karschin A (1997). Overlapping distribution of K_{ATP} channel-forming Kir6.2 subunit and the sulfonylurea receptor SUR1 in rodent brain. *FEBS Lett* **401**, 59–64.

Laughton WB & Powley TL (1987). Localization of efferent function in the dorsal motor nucleus of the vagus. *Am J Physiol* **252**, R13–R25.

Levin BE, Dunn-Meynell AA & Routh VH (1999). Brain glucose sensing and body energy homeostasis: role in obesity and diabetes. *Am J Physiol* **276**, R1223–R1231.

Levin BE, Dunn-Meynell AA & Routh VH (2001). Brain glucosensing and the K_{ATP} channel. *Nat Neurosci* **4**, 459–460.

Liss B, Bruns R & Roeper J (1999). Alternative sulfonylurea receptor expression defines metabolic sensitivity of K-ATP channels in dopaminergic midbrain neurons. *EMBO J* **18**, 833–846.

Lynch RM, Tompkins LS, Brooks HL, Dunn-Meynell AA & Levin BE (2000). Localization of glucokinase gene expression in the rat brain. *Diabetes* **49**, 693–700.

Maekawa F, Toyoda Y, Torii N, Miwa I, Thompson RC, Foster DL, Tsukahara S, Tsukamura H & Maeda K (2000). Localization of glucokinase-like immunoreactivity in the rat lower brain stem: for possible location of brain glucose-sensing mechanisms. *Endocrinology* **141**, 375–384.

Miki T, Liss B, Minami K, Shiuchi T, Saraya A, Kashima Y, Horiuchi M, Ashcroft F, Minokoshi Y, Roeper J & Seino S (2001). ATP-sensitive K^+ channels in the hypothalamus are essential for the maintenance of glucose homeostasis. *Nat Neurosci* **4**, 507–512.

Müller M, Brockhaus J & Ballanyi K (2002). ATP-independent anoxic activation of ATP-sensitive K^+ channels in dorsal vagal neurons of juvenile mice in situ. *Neuroscience* **109**, 313–328.

Oomura Y, Ono T, Ooyama H & Wayner MJ (1969). Glucose and osmosensitive neurones of the rat hypothalamus. *Nature* **222**, 282–284.

Paxinos G & Watson C (1998). *The Rat Brain in Stereotaxic Coordinates*, 4th edn. Academic Press, London.

Ritter S, Dinh TT & Zhang Y (2000). Localization of hindbrain glucoreceptive sites controlling food intake and blood glucose. *Brain Res* **856**, 37–47.

Ritter RC, Slusser PG & Stone S (1981). Glucoreceptors controlling feeding and blood glucose: location in the hindbrain. *Science* **213**, 451–452.

Rowe IC, Boden PR & Ashford ML (1996). Potassium channel dysfunction in hypothalamic glucose-receptive neurones of obese Zucker rats. *J Physiol* **497**, 365–377.

Sakura H, Ashcroft SJ, Terauchi Y, Kadowaki T & Ashcroft FM (1998). Glucose modulation of ATP-sensitive K-currents in wild-type, homozygous and heterozygous glucokinase knock-out mice. *Diabetologia* **41**, 654–659.

Singer LK & Ritter S (1996). Intraventricular glucose blocks feeding induced by 2-deoxy-D-glucose but not mercaptoacetate. *Physiol Behav* **59**, 921–923.

Song Z, Levin BE, McArdle JJ, Bakhos N & Routh VH (2001). Convergence of pre- and postsynaptic influences on glucosensing neurons in the ventromedial hypothalamic nucleus. *Diabetes* **50**, 2673–2681.

Spanswick D, Smith MA, Groppi VE, Logan SD & Ashford ML (1997). Leptin inhibits hypothalamic neurons by activation of ATP-sensitive potassium channels. *Nature* **390**, 521–525.

Spanswick D, Smith MA, Mirshamsi S, Routh VH & Ashford ML (2000). Insulin activates ATP-sensitive K^+ channels in hypothalamic neurons of lean, but not obese rats. *Nat Neurosci* **3**, 757–758.

Trapp S & Ashcroft FM (1997). A metabolic sensor in action: News from the ATP-sensitive K^+-channel. *News Physiol Sci* **12**, 255–263.

Trapp S & Ballanyi K (1995). K_{ATP} channel mediation of anoxia-induced outward current in rat dorsal vagal neurons in vitro. *J Physiol* **487**, 37–50.

Trapp S, Ballanyi K & Richter DW (1994). Spontaneous activation of K_{ATP} current in rat dorsal vagal neurones. *Neuroreport* **5**, 1285–1288.

Yang XJ, Kow LM, Funabashi T & Mobbs CV (1999). Hypothalamic glucose sensor: similarities to and differences from pancreatic beta-cell mechanisms. *Diabetes* **48**, 1763–1772.

Yang XJ, Kow LM, Pfaff DW & Mobbs CV (2004). Metabolic pathways that mediate inhibition of hypothalamic neurons by glucose. *Diabetes* **53**, 67–73.

Yettefti K, Orsini JC & Perrin J (1997). Characteristics of glycemia-sensitive neurons in the nucleus tractus solitarii: possible involvement in nutritional regulation. *Physiol Behav* **61**, 93–100.

Acknowledgements

This work was supported by an MRC Career Development Award to S.T. We thank Frances Ashcroft for the gift of SUR1 and Jonathan Lippiat for help and advice with making riboprobes.

Supplemental material

The online version of this paper can be accessed at:
DOI: 10.1113/jphysiol.2005.098822
http://jp.physoc.org/cgi/content/full/jphysiol.2005.098822/DC1
and contains supplemental material consisting of a figure entitled: Hybridisation with sense riboprobes for GLK and SUR1

This material can also be found as part of the full-text HTML version available from http://www.blackwell-synergy.com